JNCS Journal of Nepal Chemical Society January 2026, Vol. 46, No. 1, 103-111
ISSN: 2091-0304 (print)
DOI: https://doi.org/10.3126/jncs.v46i1.91127
RESEARCH ARTICLE

Hybrid α-Zirconium Phosphate/Polyaniline-Modified High-Density Polyethylene Composites with Enhanced Thermal Properties

Santosh Khanal[1]*, Mani Ram Kandel[2]

[1]*Central Department of Chemistry, Tribhuvan University, Kirtipur, Kathmandu*

[2]*Department of Chemistry, Amrit Campus, Tribhuvan University, Kathmandu*

**Corresponding E-mail:santoshkhanal2003@yahoo.com*

(Received: November 25, 2025 revised: December 24, 2025 accepted: December 29, 2025)

Abstract

Organic-inorganic hybrid nanofiller (PANI/α-ZrP) composed of polyaniline (PANI) and α-zirconium phosphate (α-ZrP) was synthesized via *in-situ* oxidative polymerization and characterized by X-ray diffraction (XRD), Fourier transform infrared spectroscopy (FTIR), Scanning electron microscopy (SEM) and thermogravimetric analysis (TGA). The α-ZrP and hybrid PANI/α-ZrP were incorporated at different weight ratios (1%, 3%, and 5%) into high-density polyethylene (HDPE) by melt mixing. Thus formed composites were characterized by X-ray diffraction and thermogravimetric analysis (TGA). The XRD results suggested that HDPE composites have mainly exfoliated and/or partially intercalated structure. Moreover, the incorporation of the hybrid fillers slightly improves the thermal stability of HDPE. The PANI/α-ZrP hybrid combines the thermal stability and flame-retardant characteristics of α-ZrP with the mechanical flexibility and interfacial compatibility of PANI, enabling better dispersion and potential reinforcement in the polymer matrix.

Keywords: Organic-inorganic hybrid; Polyaniline; Polyethylene composites; Thermal properties

Introduction

The development of polymer composites with enhanced flame retardancy and mechanical performance is vital for creating safer, more durable materials across various industries [1]. Improving the thermal and mechanical properties of polymers broadens their application range, especially in sectors demanding superior durability, fire resistance, and strength [1, 2]. Among various additives used to enhance these properties, α-zirconium phosphate (α-ZrP), a kind of layered a layered inorganic compound with the chemical formula $Zr(HPO_4)_2{\cdot}H_2O$, has attracted significant attention due to its remarkable properties such as high thermal and chemical stability, ion-exchange capacity, proton conductivity, resistance to ionizing radiation, and the ability to intercalate molecules of various sizes within its layers [3-5]. The structure of the α-ZrP consists of Zr(IV) ions situated alternately forming an octahedron with the oxygen atoms of the tetrahedral phosphate groups [6, 7].The crystalline α -ZrP possesses weak Bronsted acid and strong Lewis acid centers attributed to the P-OH group and the Zr^{4+} respectively. The surface of the α-ZrP has numerous hydroxyl group that offers surface functionalization as well [8]. The α-ZrP and its derivatives have been widely used as adsorbents, ion exchangers, drug delivery, and polymer nanocomposites [9]. Recently, α-ZrP has been widely used as flame retardant for different polymer systems. α-ZrP can reduce the heat release rate of the polymer during combustion mainly due to its physical barrier and carbonization effects [10, 11].

Polyaniline (PANI) is the most promising intrinsically conducting polymer (ICP), because of its ease of synthesis, low cost of monomer, tunable oxidation-reduction properties, better thermal and environmental stability than other ICPs [12]. It finds applications in diverse fields such as electronics, thermoelectric, sensors, capacitors and energy storage device, and wastewater treatment [13, 14]. Moreover, PANI exhibits flame retardant properties when applied to materials like cotton, polyester or cellulose fiber [15]. PANI contains amino and imine group which serve as active binding site for inorganic materials like α-ZrP to develop organic-inorganic hybrid materials. These hybrids can enhance the individual properties of both components or even introduce new functionalities due to synergistic effect, offering a promising pathway toward multifunctional materials with wide range of application [16] For instance, Wang L et al synthesized PANI/ZrP organic-inorganic hybrid by *in-situ* oxidative polymerization for the removal of model organic pollutant, methyl orange [13]. Similarly, Du X et.al developed ZrP/fibrous PANI hybrid film for the separation and recovery of Pb^{2+} ions [17]. The hybrid leverages the thermal stability and flame-retardant characteristics of α-ZrP along with the mechanical flexibility and interfacial compatibility of PANI, promoting better dispersion and potential reinforcement within the polymer matrix. To date, although PANI/α-ZrP hybrids have been synthesized, their direct incorporation into HDPE composites with the goal of simultaneously improving both thermal and mechanical properties has not been systematically explored.

Herein, we synthesized an organic–inorganic hybrid filler composed of polyaniline (PANI) andα-zirconium phosphate (α-ZrP) via *in-situ* oxidative polymerization, and incorporated it into high-density polyethylene (HDPE) using melt mixing. The hybrid nanofiller was characterized using FTIR, XRD, and SEM to confirm successful hybrid formation. The effect of PANI/α-ZrP hybrid filler on the thermal and mechanical properties of HDPE composites was evaluated by thermogravimetric analysis and tensile testing to assess their potential applications. This work provides insight into the synergistic effects of organic–inorganic hybrids in enhancing the functional performance of polymer matrices.

Materials and Methods

Chemicals

Zirconium oxychloride octahydrate ($ZrOCl_2.8H_2O$), oxalic acid anhydrous $(COOH)_2$ was obtained from Shanghai Titan Chem Co. LTD and hydrochloric acid (HCl) and phosphoric acid (H_3PO_4) was purchased from Shanghai Lingfeng chemical reagent Co. Ltd. Aniline was obtained from Shanghai Macklin Biochemical Co., Ltd. All chemicals are analytical reagent AR grade and used as received without further purification. High density polyethylene (HDPE, density: 0.93 g/cm^3; melt index: 20 g/10min @ 190 °C/2.16 kg), along with maleic anhydride grafted polyethylene (PE-g-MAH), was obtained from Fushun Petrochemical Co., Ltd., (China). α-zirconium phosphate (α-ZrP) was synthesized as previously reported method [18].

Synthesis of α-ZrP/PANI hybrid

0.016 mol of α-ZrP was dispersed in 200 mL of 1 mol L^{-1} hydrochloric acid solution. Then 0.025 mol of aniline was added drop-wise over 10 minutes with constant stirring. The resulting mixture was stirred for 24 h. 0.0312 mole of ammonium persulfate (APS) was dissolved in 20 mL of water separately and added drop-wise to the solution over 10 minutes followed by stirring for 24 h. The resulting product was filtered, washed, and dried at 80 °C for 24 h. Pure PANI was also prepared using same procedure without using α-ZrP for comparison. The mass of the obtained PANI/α-ZrP hybrid was 6.689 g. based on the masses of the hybrid and α-ZrP, the PANI content in the hybrid was calculated to be 25.3 %.

Preparation of HDPE composites

Composites of the HDPE containing α-ZrP, and PANI/α-ZrP hybrid fillers were prepared in 50 g batch using a Haake Polylab rheometer at 170 °C with a rotator speed of 50 rpm. Maleic anhydride grafted polyethylene (MA-g-PE, containing 1.96 % MA) was used as a compatibilizer at a 1:1 weight ratio relative to filler. The compositions of the composites are displayed in **Table 1**. The composites were molded into sheets by hot pressing (BL-6170-A-25J, Baolun Precision Testing Instruments Ltd., Shanghai, China) at 170 °C at a pressure of 10 MPa for 5 min, followed by cold pressing at room temperature at a pressure of 10 MPa for 5 min

Table: 1 Composition of the nanocomposites based onα-ZrP.

Sample	HDPE (g)	PE-g-MAH (g)	α-ZrP (g)	PANI/α-ZrP (g)
HD/ZrP-1	49.0	0.5	0.5	-
HD/ZrP-3	47.0	1.5	1.5	-
HD/ZrP-5	45.0	2.5	2.5	-
HD/ZrP/PANI-1	48.5	0.5		0.5
HD/ZrP/PANI-3	47.0	1.5		1.5
HD/ZrP/PANI-5	44.0	2.5		2.5

Characterization

Fourier-transform infrared (FTIR) spectra of the samples were recorded using a Nicolet 6700 spectrometer (USA) employing the KBr disc method, with 32 scans at a resolution of 4 cm^{-1} over the range of 400 to 4000 cm^{-1}. X-ray diffraction (XRD) patterns of the powder PANI/α-ZrP hybrid and thin HDPE composite sheets were obtained using a Rekagu vertical goniometer with CuKα radiation (λ = 0.154 nm) operated at 40 mA and 40 kV, scanning at a rate of 4°/min with a step size of 0.02°. The morphology of the PANI/α-ZrP hybrid was examined by scanning electron microscopy (SEM) using a Hitachi S-4800 (Japan) at an accelerating voltage of 15 kV; samples were sputter-coated with a thin layer of gold prior to imaging. Thermogravimetric analysis (TGA) was performed on a Netzsch STA 409 PC analyzer under nitrogen atmosphere (flow rate of 40 mL/min), heating samples from room temperature to 1000 °C at a rate of 10 K/min. Mechanical properties of the composites were assessed by tensile testing using a universal testing machine (MTS E 44) following the Chinese standard GB/T 1040.3–2006. Five specimens were tested for each sample, and average values were reported

Results and Discussion

The hybrid material comprising PANI and α-ZrP was synthesized through an *in-situ* oxidative polymerization approach, where aniline monomers were polymerized in the acidic medium in the presence of α-zirconium phosphate (**Scheme 1**). Initially, α-ZrP was dispersed in hydrochloric acid to promote effective interaction with the aniline. The polymerization was triggered by the drop-wise addition of ammonium persulfate as the oxidizing agent, enabling the formation of PANI chains along the surface and possibly within the interlayer spaces of the α-ZrP structure. The interaction between the PANI and α-ZrP is likely governed by hydrogen bonding and electrostatic forces between the functional groups of PANI and the phosphate groups on α-ZrP [4, 12]. The synthesized hybrid exhibited a deep greenish-black appearance, indicative of the emeraldine salt form of PANI.

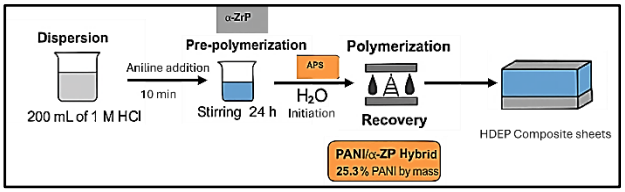

Scheme 1: Schematic diagram for the synthesis of HDPE/α-ZrP/PANI Hybrid composites.

Characterization of PANI/ α-ZrP hybrid

The morphology of the pristine PANI and PANI/α-ZrP hybrid are displayed in **Figure 1**. The α-ZrP has the layered structure [18]. The SEM image of pure PANI reveals aggregated polymer particles irregularly shaped, coarse structures, which are typical of PANI synthesized under acidic oxidation conditions. In contrast, the SEM image of PANI/ α-ZrP hybrid exhibits distinct morphological features

of both components. The lamellar or plate-like structures corresponding to α-ZrP are partially coated with the PANI matrix. This morphological integration suggests a successful hybridization process, wherein PANI has been effectively deposited onto or intercalated with the layered α-ZrP framework. The preservation of the α-ZrP layered structure in the composite indicates strong interfacial interactions between the inorganic host and the conducting polymer, which may enhance the hybrid's structural stability and functional performance [4].

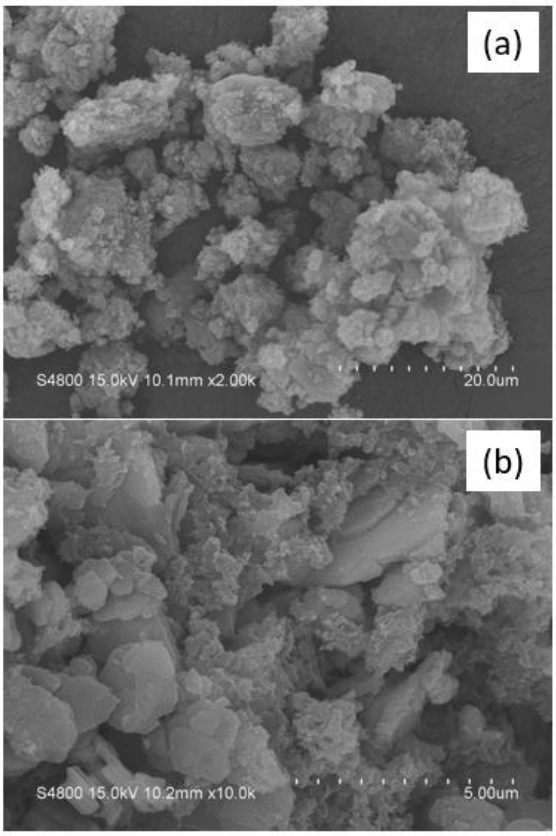

Figure 1: SEM Image of a) PANI b) α-ZrP/PANI hybrid

The chemical structure of the PANI/α-ZrP hybrid were studied using FTIR and XRD. The FTIR spectra is shown in **Figure 2(a)**. The FTIR spectra of the PANI/α-ZrP hybrid displays the characteristic peak of both PANI and α-ZrP. The strong absorption at 1560 cm^{-1} and 1477 cm^{-1} corresponds to the C=C stretching vibrations in quinoid (Q) and benzenoid (B) ring in PANI. The band at 1301 cm^{-1} and at 1244 cm^{-1} assigned to C-N and C=N stretching vibration of the PANI [3, 19]. The characteristic band of the α-ZrP is observed at 1040 cm^{-1} and 594 cm^{-1} corresponding to symmetrical stretching vibration of PO_4^{3-} and Zr-O bond, respectively [18]. The peak at 1250 cm^{-1} corresponding to P-OH stretching or deformation vibration of HPO_4^{2-} is not observed in hybrid probably due to overlap with the absorption band of PANI. The results of the FTIR suggests the successful formation of PANI/α-ZrP hybrid.

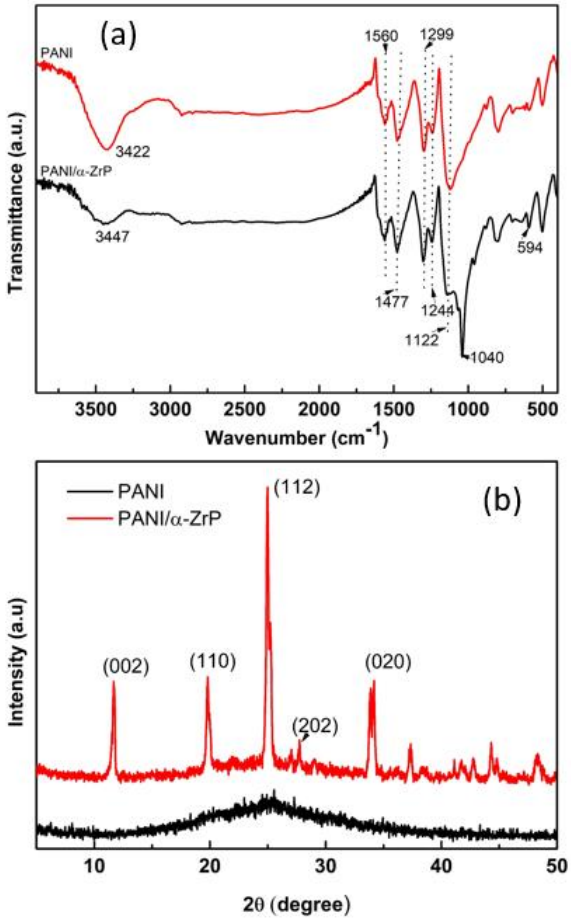

Figure 2: a) FTIR spectra b) XRD patterns of PANI/HCl and PANI/α-ZrP Hybrid.

The PANI/ α -ZrP hybrid was further characterized by using XRD analysis. The XRD diffraction patterns of the PANI and PANI/α-ZrP hybrid are shown in **Figure 2(b)**.The XRD pattern of the PANI shows board peak around 2θ of around 25° suggesting the amorphous nature of PANI. The XRD diffraction of the PANI/α-ZrP shows characteristic peaks at 2θ of 11.6 °, 19.7 ° and 24.9 ° corresponds to the diffraction peaks of (002), (110) and (112) plane

of α-ZrP, respectively [18]. The appearance of main characteristic peak of the α-ZrP in same position in hybrid indicating the crystal structure of the α-ZrP is maintained even after formation of hybrid. The position of the (002) peak in hybrid is not shifted to lower angle suggesting the formation of composite of PANI and α-ZrP instead of the intercalated PANI within the layers of α-ZrP.

The thermal properties of α-ZrP and PANI/α-ZrP hybrid was studied using thermo-gravimetric analysis. The TGA and DTG curve are shown in **Figure 3** and collected in **Table 2**.

Table 2: TGA data for α-ZrP, PANI and PANI/α-ZrP hybrid.

Sample	$T_{5\%}$ (°C)	Maximum Mass loss stage (°C)				Residue at 800 °C (%)
		T_1	T_2	T_3	T_4	
α-ZrP	125	75	167	-	597	79.1
PANI/HCl	74	66	-	236	517	39.2
PANI/ZrP	144	85	145	238	518	69.5

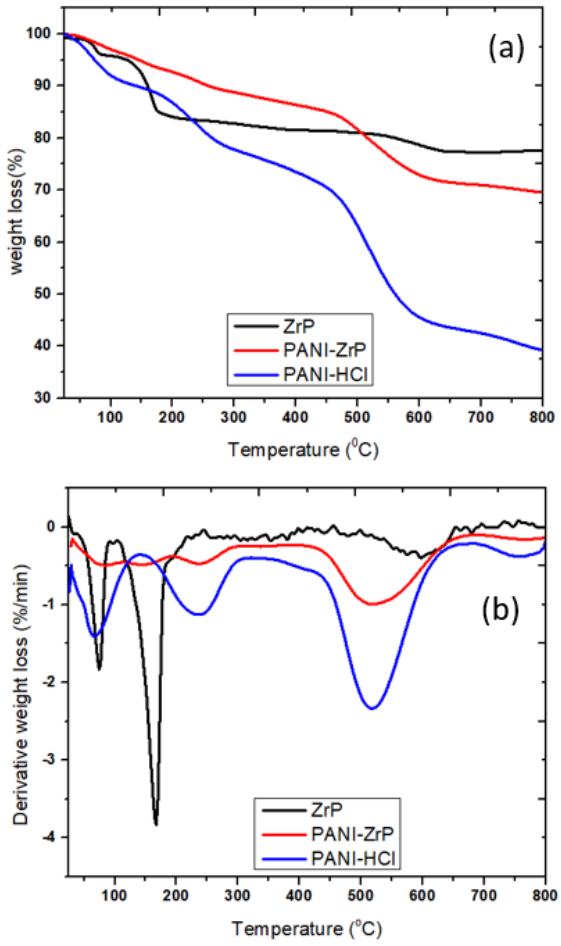

Figure 3 a) TGA and b) DTG curve for α-ZrP, PANI and, PANI/α-ZrP hybrid in nitrogen atmosphere.

The pure α-ZrP shows two major weight loss stages; the weight loss below 100 °C corresponds to weight loss due to surface moisture. The weight loss below 200 °C is due to the loss of the first level of interlayer crystallization water and the production of α-Zr $(HPO4)_2$. In final stage is due to the dehydration condensation reaction of P-OH of α-Zr $(HPO4)_2$ layer structure which generates zirconium pyrophosphate (ZrP_2O_7) [7, 8, 21]. In pure PANI, weight loss below 100 °C corresponds to loss of water molecules. The second stage is due to the elimination of dopant HCl and final stage corresponds to the thermal decomposition of the PANI backbone [22]. The PANI/α-ZrP hybrid, initial decomposition temperature (temperature of 5% weight loss $T_{5\%}$) increases as compared to pure PANI indicating higher stability of PANI due to interaction of PANI and α-ZrP. Similarly, mass loss rate is slower and char residue is higher in PANI/α-ZrP hybrid compared to that in pure PANI.

Characterization of HDPE composites

The composites of HDPE containing α-ZrP and PANI/α-ZrP hybrids (in 1 wt. %, 3 wt. % and 5 wt. %) were synthesized. The XRD diffractogram of the HDPE composites are shown in **Figure 4(a)**. The pure HDPE exhibits the diffraction angle at 2θ = 21.0° and 2θ = 21.0°.The diffraction patterns of the composites containing α-ZrP indicates that the diffraction angle corresponding to the basal spacing of the pure α-ZrP (002 plane) is shifted to the lower angle. The intensity of diffraction peak corresponds to 002 plane of α-ZrP is increased on increasing the α-ZrP content from 1% to 5%. The XRD results suggest the formation of the partially intercalated and/or exfoliated composites. The XRD patterns of the HDPE composites containing PANI/α-ZrP hybrid are shown in **Figure 4(b)**. The XRD patterns of the composites show the diffraction peak of the HDPE. The basal peak of the α-ZrP (002 plane) present in the PANI/α-ZrP hybrids appeared in the lower angle but the intensity is very low. This may suggest that the composites have

mainly exfoliated and or partially intercalated.

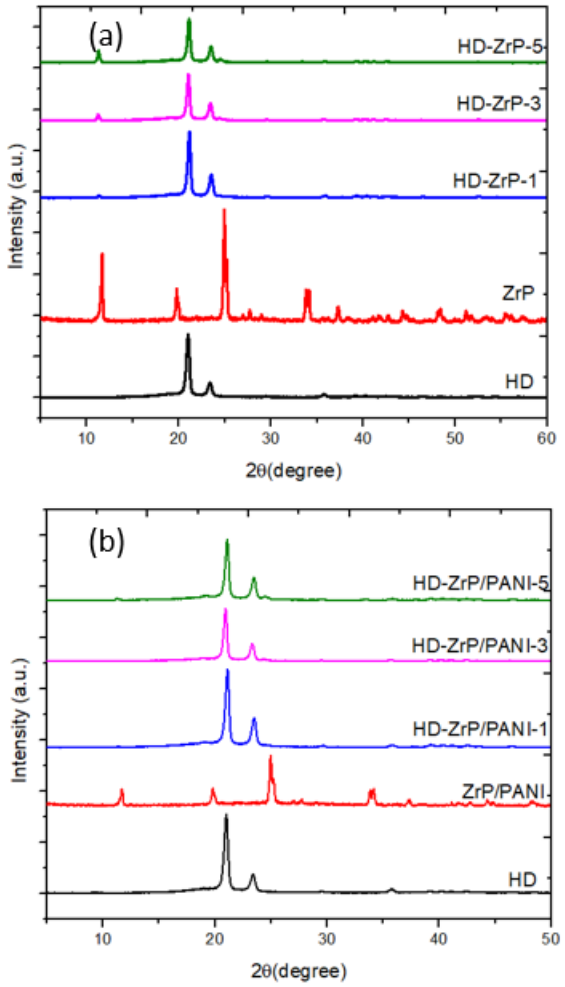

Figure 4: a) XRD patterns of the a) α-ZrP /HDPE composites b) HDPE/α-ZrP/PANI hybrid composites.

The thermal properties of the composites containing α -ZrP and PANI/ α -ZrP was determined by TGA and the results are shown in **Figure 5** and the corresponding data in **Table 3.** The temperature of onset decomposition (T_{onset}) of the composites containing α-ZrP is around 452 ^{0}C irrespective to the content of the The thermal properties of the composites containing α-ZrP and PANI/α-ZrP was determined by TGA and the results are shown in **Figure 5** and the corresponding data in **Table 3.** The temperature of onset decomposition (T_{onset}) of the composites containing α-ZrP is around 452 ^{0}C irrespective to the content of the The thermal properties of the composites containing α-ZrP and PANI/α-ZrP was determined by TGA and the results are shown in **Figure 5** and the corresponding data in **Table 3.**

Table 3: Thermal properties of the HDPE composites from TGA analysis

Sample	$T_{5\%}$ (°C)	T_{max} (°C)	MLR (%/min)	Residue at 700 °C
HD/ZrP-1	452	484	38.1	0.22
HD/ZrP-3	452	483	37.0	1.57
HD/ZrP-5	452	483	35.3	3.95
HD/ZrP/PANI-1	450	482	36.0	0.64
HD/ZrP/PANI-3	444	480	30.9	2.14
HD/ZrP/PANI-5	438	480	28.3	3.44

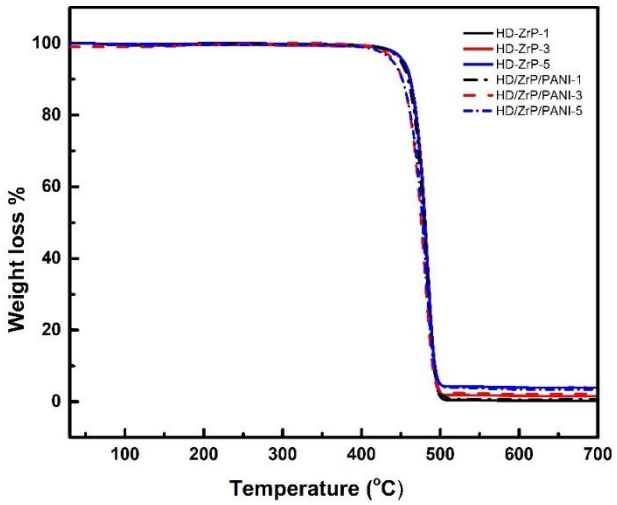

Figure 5: TGA curve of the HDPE composites containing various wt. % of α-ZrP and PANI/α-ZrP

The temperature of onset decomposition (T_{onset}) of the composites containing α-ZrP is around 452 ^{0}C irrespective to the content of the -ZrP. But in the composites containing PANI/α-ZrP hybrid, the T_{onset} is lower than that of the composites containingα-ZrP. This probably due to the decomposition of PANI present in the hybrid. When the content of the α -ZrP is increased, the mass loss rate at maximum decomposition temperature is progressively decreased, while the char residue at 700 °C is increased, indicating that the α-ZrP can delay the decomposition of the HDPE matrix and promotes the char residue. In the composites containing the PANI/α-ZrP hybrid, the mass loss rate is even lower compared with same content of the α-ZrP. The results of the TGA indicates that the thermal stability of the HDPE is enhanced on addingα-ZrP and PANI/α-ZrP hybrid, with hybrid perform little better.. But in

the composites containing PANI/α-ZrP hybrid, the T_{onset} is lower than that of the composites containing α-ZrP. This probably due to the decomposition of PANI present in the hybrid. When the content of the α-ZrP is increased, the mass loss rate at maximum decomposition temperature is progressively decreased, while the char residue at 700 °C is increased, indicating that the α-ZrP can delay the decomposition of the HDPE matrix and promotes the char residue. In the composites containing the PANI/α-ZrP hybrid, the mass loss rate is even lower compared with same content of the α-ZrP. The results of the TGA indicates that the thermal stability of the HDPE is enhanced on addingα-ZrP and PANI/α-ZrP hybrid, with hybrid perform little better.. But in the composites containing PANI/α-ZrP hybrid, the T_{onset} is lower than that of the composites containing α-ZrP. This probably due to the decomposition of PANI present in the hybrid. When the content of the α-ZrP is increased, the mass loss rate at maximum decomposition temperature is progressively decreased, while the char residue at 700 °C is increased, indicating that the α-ZrP can delay the decomposition of the HDPE matrix and promotes the char residue. In the composites containing the PANI/α-ZrP hybrid, the mass loss rate is even lower compared with same content of the α-ZrP. The results of the TGA indicates that the thermal stability of the HDPE is enhanced on adding α-ZrP and PANI/α-ZrP hybrid, with hybrid perform little better.

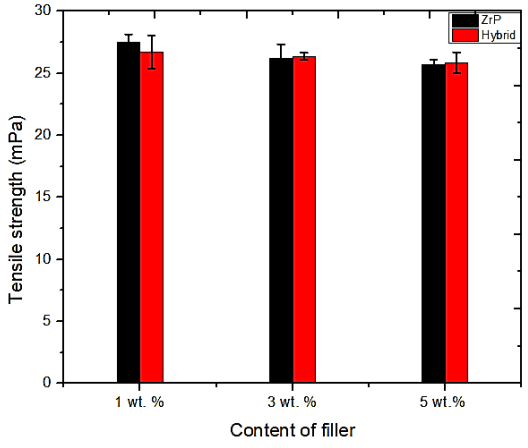

Figure 6: Tensile strength of the HDPE composites

The tensile properties of the HDPE composites containing α-ZrP and its hybrid with PANI was measured. The results are shown in **Figure 6**. The tensile strength of the HDPE used in this study is measured as 26.5 ± 0.5 mPa. The tensile strength of the nanocomposites has not significantly changed on adding both α-ZrP and its hybrid.

Conclusions

An organic–inorganic hybrid filler based on polyaniline (PANI) and α-zirconium phosphate (α-ZrP) was successfully synthesized via in-situ oxidative polymerization and incorporated into HDPE via melt mixing. FTIR, XRD, and SEM confirmed the formation and dispersion of the hybrid, showing granular PANI embedded within the layered α-ZrP structure. XRD analysis of the composites indicated partially intercalated/exfoliated morphology. While tensile strength showed minimal change, thermogravimetric analysis revealed improved thermal stability and char yield, particularly for PANI/α-ZrP-filled composites. These results suggest that PANI/α-ZrP hybrids can act as effective flame-retardant additives in HDPE systems. Future work will focus on optimizing filler content and exploring multifunctional applications.

Acknowledgements

Authors would like to acknowledge Professor Shiai Xu of School of Materials Science and Engineering, East China University of Science and Technology, Shanghai, China for support and laboratory facilities.

Author's contribution statement

S. Khanal: Conceptualization, Methodology, Investigation, Formal analysis, Data curation, Writing-original draft preparation, Writing-review and editing, **M. R. Kandel:** Conceptualization, Formal analysis, Data curation, Writing-review and Editing

Conflict of interest

The authors declare no conflict of interest.

Data availability statement

The data that supports the findings of this

study can be made available from the corresponding author, upon reasonable request.

References

1. E. V. Bachtiar, K. Kurkowiak, L. Yan, L., B. Kasal, and T. Kolb,Thermal stability, fire performance, and mechanical properties of natural fibre fabric-reinforced polymer composites with different fire retardants, *Polymers*, 2019, *11*(4), p.699. (DOI: 10.3390/polym11040699)
2. O.A. Afolabi, and N. Ndou, Synergy of hybrid fillers for emerging composite and nanocomposite materials—a review. *Polymers*, 2024 16(13), p.1907. (DOI: https://doi.org/10.3390/polym16131907)
3. Z. Lv, K. Ren, T. Liu, Y. Zhao, Z. Zhang, Z. and G. Li, Design polyaniline/α-zirconium phosphate composites for achieving self-healing anti-corrosion of carbon steel. *Nanomaterials*, 2023 *14*(1), p.76. (DOI: https://doi.org/10.3390/nano14010076)
4. M. Pica, Treatment of wastewaters with zirconium phosphate based materials: A review on efficient systems for the removal of heavy metal and dye water pollutants. *Molecules*, 2021, *26*(8), p.2392. (DOI: 10.3390/molecules26082392)
5. H. Ding, A. Ahmed, K. Shen, K. and L. Sun, Assembly of exfoliated α - zirconium phosphate nanosheets: Mechanisms and versatile applications: Nanoscience: Special Issue Dedicated to Professor Paul S. Weiss. *Aggregate*, 2022, *3*(4), p.e174 (DOI: https://doi.org/10.1002/agt2.174)
6. D. Capitani, M. Casciola, A. Donnadio, A. and R. Vivani, High yield precipitation of crystalline α-zirconium phosphate from oxalic acid solutions. *Inorganic chemistry*, 2010, *49*(20), 9409-9415. (DOI: https://doi.org/10.1021/ic101200f)
7. C. Trobajo, S. A. Khainakov, A. Espina, and J. R. García, On the synthesis of α-zirconium phosphate. *Chemistry of materials*, 2000, *12*(6), 1787-1790. (DOI: https://doi.org/10.1021/cm0010093)
8. H. Karimi, H., Preparation of zirconium phosphate nanoparticles and its application in the protection of aldehydes, *Journal of Sciences, Islamic Republic of Iran*, 2017, *28*(4), pp.313-323.
9. Z. Ye, L. Chen, H. Chen, L. Han, L., Q. Chen, and D. Wang, D., α-Zirconium phosphate nanocrystals with various morphology for photocatalysis, *Chemical Physics Letters*, 2018, *709*, 96-102. (DOI: 10.1016/j.cplett.2018.08.046)
10. B. Xu, W. Xu, Y. Liu, R. Chen, W. Li, Y. Wu, and Z. Yang, Surface modification of α - zirconium phosphate by zeolitic imidazolate frameworks - 8 and its effect on improving the fire safety of polyurethane elastomer, *Polymers for Advanced Technologies*, 2018. *29*(11), 2816-2826. (DOI: https://doi.org/10.1002/pat.4404)
11. H. Xiao, and S. Liu, Zirconium phosphate (ZrP)-based functional materials: Synthesis, properties and applications. *Materials & Design*, 2018, *155*, 19-35. (DOI: 10.1016/j.matdes.2018.05.041
12. M. L. Mota, A. Carrillo, A. J. Verdugo, A. Olivas, J. M. Guerrero, E. C. De la Cruz, and N. Noriega Ramírez, Synthesis and novel purification process of PANI and PANI/AgNPs composite. *Molecules*, 2019, *24*(8), p.1621. (DOI: 10.3390/molecules24081621
13. L. Wang, X. L.Wu, W. H. Xu, X. J Huang, J. H. Liu, and A. W. Xu, Stable organic–inorganic hybrid of polyaniline/α-zirconium phosphate for efficient removal of organic pollutants in water environment. *ACS applied materials & interfaces*, 2012 *4*(5), 2686-2692. (DOI: https://doi.org/10.1021/am300335e)
14. M. R. Devi, A. Saranya, J. Pandiarajan, J. Dharmaraja, N. Prithivikumaran, and N. Jeyakumaran, Fabrication, spectral characterization, XRD and SEM studies on some organic acids doped polyaniline thin films on glass substrate, *Journal of King Saud University-Science*, 2019, *31*(4),1290-1296.
15. X. Wu, X. Qian, X. and X. An, Flame retardancy of polyaniline-deposited paper composites prepared via in situ polymerization, *Carbohydrate polymers*, 2013, *92*(1), pp. 435-

440
(DOI: 10.1016/j.carbpol.2012.09.032)

16. A. F. Baldissera, J. F Souza, J.F. and C. A Ferreira, Synthesis of polyaniline/clay conducting nanocomposites.*Synthetic metals*, 2013, *183*, pp.69-72. (DOI: 10.1016/j.synthmet.2013.09.022)
17. X. Du, Q. Zhang, W. Qiao, X. Sun, X. Ma, X. Hao, Z. Wang, A. Abudula, and G. Guan, Controlled self-assembly of oligomers-grafted fibrous polyaniline/single zirconium phosphate nanosheet hybrids with potential-responsive ion exchange properties. *Chemical Engineering Journal*, *302*, 2016, 516-525. (DOI:10.1016/j.cej.2016.05.066)
18. S. Khanal Y. Lu L. Dang, M. Ali M and S. Xu S, Effects of α-zirconium phosphate and zirconium organophosphonate on the thermal, mechanical and flame retardant properties of intumescent flame retardant high density polyethylene composites. *RSC Advances*, 2020, 10, 30990-31002. (DOI: 10.1039/d0ra04929h)
19. Z. Zhang, Y. Han, T. Li, T. Wang, X. Gao, Q. Liang, and L. Chen, 2016. Polyaniline/montmorillonite nanocomposites as an effective flame retardant and smoke suppressant for polystyrene, *Synthetic Metals*, 2016, *221*, 28-38. (DOI:10.1016/j.synthmet.2016.10.009)
20. G. Madhu, H. Bhunia, P.K. Bajpai, and V. Chaudhary, Mechanical and morphological properties of high density polyethylene and polylactide blends. *Journal of Polymer Engineering*, 2014, *34*(9), 813-821. (DOI: 10.1515/polyeng-2013-0174)
21. L. Han, Q. Chen, H. Chen, S. Yu, L. Xiao, and Z. Ye, Synthesis and Performance of Functionalized α - Zirconium Phosphate Modified with Octadecyl Isocyanate, *Journal of Nanomaterials*, *2018* (1), 5873871. (DOI: https://doi.org/10.1155/2018/5873871)
22. S. Kazim, S. Ahmad, J. Pfleger, J. Plestil, and Y. M. Joshi, Polyaniline–sodium montmorillonite clay nanocomposites: effect of clay concentration on thermal, structural, and electrical properties. *Journal of Materials Science*, 2012, *47*, 420-428. (DOI: 10.1007/s10853-011-5815-y)